Development of characteristics of laterite soil-based mixtures for the removal of nitrate from drinking water

P.G.H. Pupulewatte, N.U.S. Dissanayake*, D.T. Jayawardana, B.M. Gunathilake, A.V.P.S. Buddhima

Department of Forestry and Environmental Science, Faculty of Applied Sciences, University of Sri Jayewardenepura, Gangodawila, Nugegoda, Sri Lanka, Tel.: +94 715277235; email: sandalidissanayake@sci.sjp.ac.lk (N.U.S. Dissanayake), Tel.: +1 7328617459; email: heshpupulewatte@gmail.com (P.G.H. Pupulewatte), Tel.: +94 778802631; email: daham@sci.sjp.ac.lk (D.T. Jayawardana), Tel.: +94 71720 9917; email: bhanukagunathilake@sjp.ac.lk (B.M. Gunathilake), Tel.: +94 71383 4676; email: sandaniv@sci.sjp.ac.lk (A.V.P.S. Buddhima)

ABSTRACT

The main objective of this study is to investigate surface adsorption characteristics and physical conditions of laterite for the removal of nitrate in aqueous solutions with the appropriate amendment for the effective removal of nitrate from drinking water. The physico-chemical properties of laterite soil were analyzed. The effects of various operational parameters such as solution pH, adsorbent dosage, contact time, and the initial concentration of nitrate were examined on nitrate adsorption by laterite and laterite-limestone soil mixtures using the batch experiments. The obtained results showed that the maximum percentage of nitrate adsorption attained by raw laterite was at initial pH 3, after 60 min of contact time, and with an adsorbent dose of 2 g. Pseudo-first-order kinetic model and Langmuir isotherm model showed the best fit for the experimental adsorption data, and a maximum adsorption capacity of 0.628 mg/g was observed. Laterite-limestone mixture containing 60% laterite showed the highest removal efficiency. The results obtained by the limestone-laterite mixture showed that the maximum removal efficiency attained was at pH 3, after 180 min of contact time, and with an adsorbent dose of 2 g. Although the optimum pH was similar in both soil samples, the final pH of the solution had increased to 6.75 ± 0.17. Pseudo-second-order kinetic model and Freundlich isotherm model showed the best fit for the experimental adsorption data. This soil mixture was used to determine the effect of competing anions on the nitrate removal efficiency. It was found that phosphate ions have shown maximum influence.

Keywords: Laterite; Adsorption; Nitrate; Limestone

1. Introduction

In many parts of the world, groundwater serves as the sole source of drinking water in rural communities and urban areas. However, in recent years, increased industrial and agricultural activities have resulted in the generation of toxic pollutants. Inorganic pollutants are necessary since, even at low concentrations, they are unhealthy and harmful to humans and animals. As there are usually no organoleptic changes in drinking water due to trace levels of toxic inorganic anions, these ions may remain undetected, thereby increasing the possible health risks caused by them [1].

Many inorganic anions have been found in potentially harmful concentrations in numerous drinking water sources. Of these, nitrate is of prime concern on a global scale. Nitrate is a naturally occurring ion in the nitrogen

* Corresponding author.

cycle that is the stable form of nitrogen (N) for oxygenated systems. Due to its high-water solubility [2], it is possibly the most widespread groundwater contaminant globally [3].

Since the 1920s, human activities have doubled the natural rate of nitrogen deposited onto land. The main reason for this is the significant rise in nitrate-based chemical fertilizers. Other than that, decaying vegetable, animal, and human waste, domestic effluents (sewage sludge disposal and industrial discharge), precipitation, atmospheric washout, septic systems, pesticides, and waste contamination through storm and urban runoff are also significant sources of nitrate [4]. In recent years, groundwater contamination by nitrate has been documented all over the world, including in countries such as Sri Lanka [5], India [6], and China [7].

High nitrate concentrations in drinking water sources can lead to a potential environmental and public health risk. They stimulate heavy algal growth, thus promoting eutrophication in water bodies. In humans, increasing nitrate concentrations in drinking water causes adverse health effects such as induction of methemoglobinemia, the potential formation of carcinogenic nitrosamines, and adverse reproductive outcomes [8]. Due to problems associated with excess nitrate concentrations in drinking water, the World Health Organization has set a maximum contaminant level of 10 mg/L of nitrate in drinking water [9].

Water must be treated to meet these guidance limits to meet regulated concentrations. However, it is almost impossible to remove nitrate by conventional drinking water treatment methods due to high stability and solubility of nitrate [3,4]. The most commonly used treatment methods to remove/reduce nitrate include chemical denitrification using zero-valent iron (Fe_0), zero-valent magnesium (Mg_0), ion exchange, reverse osmosis, electrodialysis, catalytic denitrification, and biological denitrification. However, these technologies have their strengths and limitations and are expensive, less effective, and generate additional by-products [5]. Therefore, the search for efficient, effective, and less costly methods to remove nitrate from drinking water remains open. The adsorption process is generally considered better in water treatment because of convenience, ease of operation, and simplicity of design. Further, it has broader applicability in water pollution control, uses very simple technology, and has higher efficiency in removing water contaminants [3,5].

Laterite is usually defined as a relatively dense, earthy mass that is enriched in iron and aluminum hydroxides and dries relatively rapidly in the air. In addition to minerals of the aluminum and iron hydroxide groups, laterite contains considerable amounts of kaolinite, filling the cells of the kaolinite-sesquioxide matrix [10]. Laterite soil contains SiO_2, Fe_2O_3, Al_2O_3, which can create both positive and negative charges on the surface of laterite at neutral pH. This makes laterite a good adsorbent. Other than that, the high porosity and the availability of anion exchange sites are advantageous for the use of laterite as an adsorbent [11,12]. Through studies, it can be seen that laterite has shown positive results in the removal of anions such as fluoride [13–15], phosphate [15,16], arsenite [12], and heavy metals such as copper [17,18], lead and chromium [11,18].

Crystalline limestones, which are also known as marbles, cover about 30% of the land area of Sri Lanka [19]. Major

minerals found in marble are calcite and dolomite. Out of them, most marbles contain dolomite as a major mineral with variable other compositions [19,20]. These rocks have a high industrial potential due to their wide distribution in rural areas. However, currently, Sri Lankan marbles are only used for construction activities and in the industries of lime and fertilizer.

Limestone is one of the most suitable candidates for acidic water neutralization as well as for the removal of a number of pollutants. Limestone is a commercial material for acidic neutralization of water and agriculture grounds [21]. The advantage of using limestone is due to the fact that calcium-based materials have shown that they are highly usable materials in water purification, especially for contaminant removal technologies. $CaCO_3$ is a good material for arsenic [22], industrial dye [21], iron, and manganese [23] removal from drinking water. As a result, removing nitrate through adsorption using a laterite-based filter may be a convenient, effective, and worthwhile solution to the problem of nitrate contamination in groundwater. Since laterite soil has special qualities that make nitrate removal using it effective. It offers a sustainable and environmentally friendly solution that can be implemented in both rural and urban areas to ensure that communities have access to clean and safe water. Laterite soil is a natural filter medium that can be used for nitrate removal and is widely available and affordable. The aim of the study is to investigate the surface adsorption characteristics and physical conditions of laterite, and develop laterite soil mixtures that can be used to remove nitrate from aqueous solutions. For this purpose, the laterite/limestone composite was synthesized and a detailed analysis of structure was described. Prepared and characterized materials were tested for removal of nitrates from aqueous solutions.

2. Material and methods

2.1. Materials

The laterite material obtained from the southwestern part of Sri Lanka was washed several times using distilled water to remove earthy impurities, air-dried, ground, and sieved using a 0.5 mm US Standard. To minimize the contamination and moisture loss, soil samples were taken as composite and collected in polyethylene zip lock bags.

Nitrate, sulfate, chloride, and phosphate solutions were prepared by dissolving sodium nitrate ($NaNO_3$), sodium fluoride (NaF), potassium phosphate dibasic anhydrous (K_2HPO_4) in distilled water. All chemicals and solvents used during experiments were of analytical grade quality.

2.2. Laterite/limestone powder composite production

Laterite and limestone powder were mixed at different mass percentages ranging from 50% to 100% with respect to laterite while keeping the total mass a constant at 1.00 g. A series of nitrate solutions (C_0 = 25 mg/L) were added to the prepared mixtures keeping a ratio of [m:V] = [1:50]. The mixtures were then shaken for 24 h with an agitation speed 120 rpm at room temperature. The solid phase was separated by centrifugation at 4,000 rpm for 10 min. The solutions were filtered by a millex-GP syringe filter unit pore size

0.22 μm. The concentration of remaining nitrate was determined in supernatants by the Hach DR900 Multiparameter Portable Colorimeter. The percentage removal efficiency was calculated using Eq. (1).

$$\text{Percentage Removal Efficiency} = \frac{\left(C_0 - C_e\right)}{C_0} \times 100 \quad (1)$$

where C_0 and C_e are initial and equilibrium concentrations of nitrate in solution (mg/L).

The amount of nitrate absorbed per unit weight of adsorbent (q_e in mg/g) was calculated as Eq. (2).

$$\text{Adsorption capacity} = \frac{\left(C_0 - C_e\right) \times V}{m} \quad (2)$$

where C_0 and C_e are initial and equilibrium concentrations of nitrate in solution (mg/L), V is the volume of solution (L), and m is the mass of the laterite (g) [11,24].

2.3. Physico-chemical analyses

The soil samples were analyzed for available major and trace elements by X-ray fluorescence spectrometry using the Rigaku NEX CG EDXRF analyzer. Splits of each sample were oven-dried for 48 h at 160°C. Powdered samples were compressed into briquettes under a force of 200 kN for 60 s [25].

The powdered sample was analyzed for specific surface area and pore size distributions by N_2 adsorption at 77 K using the Autosorb iQ-MP-(1STAT) Viton BET surface area analyzer. Parameters of the instrument were set according to 12.4 h of approximate outgas time, and 300°C final outgas temperature Analysis was carried out for 3.25 h using the standard analysis mode.

Fourier-transform infrared spectroscopy (FTIR) analysis was used to identify and study the behavior of adsorption sites in laterite soil. Thus, investigations were carried out using the Nicolet iS10 spectrometer before and after the adsorption, using the KBr-pellet method, and spectra were obtained between 4,000–400 cm^{-1} [15,18,26].

The pH of the soil suspension solutions (1:5 = soil:water) was measured using WTW ProfiLine pH 3110 pH Meter with ±0.005 variations. pH values were measured by means of the wet sediment analysis method.

2.3.1. Determination of the pHzpc of laterite

For the determination of the pH value at the point of zero charges of laterite, solutions of 50 mL 0.1 M NaCl was taken, and the initial pH (pH$_i$) of solutions was adjusted between 2 and 10 by the addition of 0.1 M HCl and 0.1 M NaOH. After pH adjustment, 0.05 g laterite was added to the solutions, and the suspension was shaken at a speed of 120 rpm at room temperature. After 24 h, the solutions were filtered by a 0.22 μm cellulose acetate membrane, and the filtrates' final pH (pH$_f$) was measured. The difference between the initial and final pH values (ΔpH = pH$_i$ − pH$_f$) was plotted vs. pH$_i$. The pH at which ΔpH = 0 was considered the pH value at the point of zero charges [12,13].

2.3.2. Elution analyses to study water-soluble fraction

Since there can be accumulated metal ions readily available in laterite soil samples, those metal ion concentrations were analyzed. 10 g laterite samples were dissolved in 50 mL of distilled water, maintaining a ratio of 1:5, and were stirred for 2 h. After 2 h, the solid phase was separated by using centrifugation (4,000 rpm) for 10 min, and then solutions were filtered by a millex-GP syringe filter unit pore size 0.22 μm. The filtrate was acidified using concentrated HCl for preservation and further analysis. The prepared samples were analyzed for metal ion concentrations using the Agilent 7900 ICP-MS.

2.4. Batch adsorption studies

2.4.1. Effect of solution pH

The pH of the solution dramatically affects adsorption studies, and it can affect the surface charge, dissociation of functional groups of the adsorbent, chemical speciation, and diffusion rate of solute [27]. The initial pH of aqueous nitrate solution with C_0 = 25 mg/L was adjusted to pH 2–11 by using 0.1 M HCl and 0.1 M NaOH. Then the required amount of material was added to the solution, maintaining 1:50 (used units for ratio g:mL) ratio of soil and the nitrate solution, respectively. The mixture was shaken at 120 rpm at 25 at room temperature for 24 h. After 24 h, the solid phase was separated by using centrifugation at 4,000 rpm for 10 min, and then solutions were filtered by millex-GP syringe filter unit pore size 0.22 μm. The concentration of remaining nitrate was determined in supernatants immediately by the Hach DR900 Multiparameter Portable Colorimeter. This procedure was carried out for both raw laterite (RL) and 60% raw laterite and 40% limestone mixture (LD60) samples.

2.4.2. Effect of adsorbent dosage

The effect of adsorbent dosage on nitrate adsorption was studied by adjusting the solution pH at optimum with an initial nitrate concentration of 25 mg/L and by adding the varying adsorbent dosage ranging from 0.50 to 10.00 g. The mixtures were shaken at a speed of 120 rpm using a shaking assembly at room temperature for 24 h. Then the solid phase was separated by using centrifugation at 4,000 rpm for 10 min, and then solutions were filtered by millex-GP syringe filter unit pore size 0.22 μm. The concentration of remaining nitrate was determined in supernatants by the Hach DR900 Multiparameter Portable Colorimeter. This procedure was carried out for both RL and LD60 samples [24].

2.4.3. Adsorption kinetic studies

The influence of contact time on adsorption experiments was investigated. The series of solutions with an initial nitrate concentration of 25 mg/L were mixed with soil maintaining 1:50 ratio of soil and nitrate solution, respectively, at optimum pH. The mixtures were then shaken in time intervals from 5 min to 24 h with an agitation speed 120 rpm at room temperature, followed by solid-phase separation by centrifugation at 4,000 rpm for 10 min. The solutions were filtered by millex-GP syringe filter unit pore size of 0.22 μm. The concentration of remaining nitrate was determined in

supernatants by the Hach DR900 Multiparameter Portable Colorimeter. This procedure was carried out for both RL and LD60 samples. The percentage removal efficiency and the amount of nitrate absorbed per unit weight of adsorbent were calculated using Eqs. (1) and (2), respectively [11,24]. The rate of adsorption can be predicted by kinetic adsorption parameters. This factor is important and useful in predicting the adsorption mechanism [11,24]. The dynamics of the nitrate adsorption process by RL and LD60 were evaluated with the pseudo-first-order [Eq. (3)] [28], pseudo-second-order [Eq. (4)] [29], intraparticle diffusion [Eq. (5)] [9] kinetic models. The non-linear forms of these models:

$$q_t = q_e \left(1 - e^{-k_1 t}\right) \tag{3}$$

$$q_t = \frac{q_e^2 k_2 t}{1 + q_e k_2 t} \tag{4}$$

$$q_t = K_p t^{1/2} + I \tag{5}$$

where q_t and q_e and are the amounts of nitrate ions adsorbed on the modified biochar (mg/g) at time t and equilibrium time, respectively; k_1 is the rate constant of the pseudo-first-order (min^{-1}), k_2 is the rate constant of the pseudo-second-order (g/mg·min); K_p is the intraparticle diffusion rate constant (mg/g·min$^{1/2}$) and I (mg/g) is the intercept of the intraparticle diffusion model.

2.4.4. Adsorption equilibrium studies

Equilibrium adsorption experiments were conducted by taking a series of solutions with initial nitrate concentrations of 5–30 mg/L with an optimum solution pH and optimum adsorbent at room temperature. The mixtures were shaken at 120 rpm, and after equilibration, samples were filtered by 0.22 μm cellulose acetate membrane filters and were analyzed by the Hach DR900 Multiparameter Portable Colorimeter for the determination of residual nitrate concentration. Equilibrium data are important requirements for the successful modeling of adsorption systems. There are different theoretical and empirical relationships for the modeling of the adsorption process [24]. In this study, Langmuir, Freundlich, and Temkin models were applied to describe the adsorption process, and the equations used [30–32].

$$q_e = \frac{Q_0 K_L C_e}{1 + K_L C_e} \tag{6}$$

$$\frac{C_e}{q_e} = \frac{1}{Q_0 K_L} + \frac{1}{Q_0} C_e \tag{7}$$

where C_e = the equilibrium concentration of adsorbate (mg/L), q_e = the amount of solute adsorbed per gram of the adsorbent at equilibrium (mg/g), Q_o = maximum monolayer coverage capacity (mg/g), K_L = Langmuir isotherm constant (L/mg).

$$q_e = K_F C_e^{1/n_f} \tag{8}$$

$$\ln q_e = \frac{1}{n_f} \ln C_e + \ln K_F \tag{9}$$

where q_e = the amount of solute adsorbed per unit weight of adsorbent (mg/g), C_e = the equilibrium concentration of adsorbate (mg/L), K_F = Freundlich constant indicative of the relative adsorption capacity of the adsorbent (mg/g), $1/n_f$ = the heterogeneity factor.

$$q_e = \frac{RT}{b_T} \ln A_T + \frac{RT}{b_T} \ln C_e \tag{10}$$

where q_e = the amount of solute adsorbed per unit weight of adsorbent (mg/g), C_e = the equilibrium concentration of adsorbate (mg/L), A_T = Temkin isotherm equilibrium binding constant (L/g), b_T = Temkin isotherm constant, R = is universal gas constant (8.314 J/mol·K), T = temperature (298 K).

2.4.5. Effect of competing ions

The adsorption capacity of LD60 for nitrate adsorption in the presence of co-existing (competing) anions (e.g., phosphate, sulfate, and fluoride), which are commonly present in real groundwater, was investigated. Experiments were conducted by adding varying concentrations of co-existing anions (5, 10, 15, 20, and 25 mg/L) in nitrate solution of fixed nitrate concentration of 25 mg/L, optimum pH, and optimum adsorbent dosage. The mixtures were shaken at a speed of 120 rpm at room temperature for their optimum time. Then the solid phase was separated from the solution by filtration using a millex-GP syringe filter unit pore size 0.22 μm. The concentration of remaining nitrate was determined in supernatants by the Hach DR900 Multiparameter Portable Colorimeter. This procedure was carried out for the final mixture of LD60 [24].

2.5. Analysis of real drinking water samples

Groundwater samples were collected from Jaffna, Sri Lanka, which is known to have high nitrate contamination [33,34]. The initial nitrate concentration of collected samples was measured. LD60 was used as the adsorbent. For 50 mL of groundwater, 2.00 g of LD60 was added, and the pH was adjusted to 3 using 0.1 M HCl and 0.1 M NaOH. The mixtures were shaken at a speed of 120 rpm at room temperature for 180 min. Then solid phase was separated from the solution by filtration using millex-GP syringe filter unit with a pore size 0.22 μm. The concentration of remaining nitrate was determined in supernatants by the Hach DR900 Multiparameter Portable Colorimeter. The percentage removal efficiency was calculated using Eq. (1) [24].

2.6. Analysis of data

All analyses were performed using IBM SPSS Statistics 18.

3. Results and discussion

3.1. Physico-chemical analysis of mixture

The X-ray fluorescence analysis was performed to identify the composition of soil sample (Table 1). For laterite, 33 elements and compounds were identified. In all the samples,

Table 1
Composition of raw laterite

	No. 1	No. 2	No. 3	Avg.	Min.	Max.	SD
Mineral oxides/wt.%							
SiO_2	44.60	44.30	44.80	44.60	44.30	44.80	0.25
Al_2O_3	32.90	33.50	33.00	33.10	32.90	33.50	0.32
Fe_2O_3	19.30	18.80	18.90	19.00	18.80	19.30	0.26
TiO_2	2.31	2.34	2.33	2.33	2.31	2.34	0.02
K_2O	0.17	0.17	0.16	0.17	0.16	0.17	0.005
CaO	0.08	0.07	0.09	0.08	0.07	0.09	0.01
Elements/wt.%							
Fe	64.80	64.60	65.80	65.10	64.60	65.80	0.64
Al	16.30	15.80	15.80	16.00	15.80	16.30	0.29
Si	14.90	15.60	14.70	15.10	14.70	15.60	0.47
Ti	1.91	1.91	1.87	1.90	1.87	1.91	0.02
Zr	1.00	0.98	1.00	0.99	0.98	1.00	0.009
Tb	0.26	0.20	0.35	0.27	0.20	0.35	0.08
Co	0.18	0.20	0.20	0.19	0.18	0.20	0.01
Gd	0.18	0.16	0.00	0.17	0.16	0.18	0.008
K	0.13	0.13	0.13	0.13	0.13	0.13	0.001
V	0.08	0.09	0.09	0.09	0.08	0.09	0.002

Table 2
Composition of raw limestone

	No. 1	No. 2	No. 3	Avg.	Min.	Max.	SD
Mineral oxides/wt.%							
CaO	73.60	59.10	58.30	63.80	58.30	73.60	8.61
MgO	20.40	35.80	36.40	30.90	20.40	36.40	9.07
SiO_2	4.34	3.58	3.74	3.89	3.58	4.34	0.40
Fe_2O_3	0.41	0.60	0.58	0.53	0.41	0.60	0.11
SO_3	0.45	0.38	0.41	0.41	0.38	0.45	0.04
Al_2O_3	0.19	0.11	0.16	0.16	0.11	0.19	0.04
K_2O	0.05	0.03	0.02	0.03	0.02	0.05	0.01
Elements/wt.%							
Si	1.79	1.79	1.73	1.77	1.73	1.79	0.035
Fe	0.47	0.43	0.54	0.48	0.43	0.54	0.056
Zr	0.34	0.35	0.35	0.35	0.34	0.35	0.006
S	0.14	0.14	0.15	0.14	0.14	0.15	0.004
Al	0.05	0.05	0.05	0.05	0.05	0.05	0.001
K	0.02	0.02	0.02	0.02	0.02	0.02	0.001
Mn	0.02	0.02	0.01	0.01	0.01	0.02	0.008
Eu	0.01	0.02	0.09	0.04	0.01	0.09	0.043
Cu	0.02	0.01	0.01	0.01	0.01	0.02	0.002

Fe was the most common element, with an average mass percentage of 65.1% ± 0.64%. Other than that Al, and Si were also abundant. SiO_2 was the most abundant in all three compounds. Al_2O_3 and Fe_2O_3 were also present in high amounts. Other detected compounds include TiO_2, CaO, and K_2O. In limestone, 22 elements and compounds were identified (Table 2). CaO is the most abundant in all three compounds, with an average of 63.67% ± 8.61%. MgO and SiO_2 were also present in high amounts. Heavy metals were only present in minute amounts. Therefore, if they were eluted, the concentration would be very low.

FTIR was used to identify the functional groups and molecular structures in a soil sample. In the OH stretching vibration region (3,700–3,300 cm^{-1}), the FTIR spectra (Fig. 1) shows five absorption bands at 3,695; 3,649; 3,618; 3,448 and 3,525 cm^{-1} [14]. The stretching modes of OH bands related to free water (around 3,600 cm^{-1}) and the bending mode of H–O–H band were also observable (around 1,643 cm^{-1}). The band at 3,695 cm^{-1} can be attributed to stretching vibrations of outer hydroxyl groups coordinated to iron, aluminum or silica present in laterite [35], and the band at 3,618 cm^{-1} can be associated with inner hydroxyl groups. The absorption band near 3,400 cm^{-1} is reported by the hydroxyl bonded to trivalent cations such as Al^{3+} or Fe^{3+}. Therefore, the bands at 3,525; 3,448 and 3,379 cm^{-1} indicate some portion of Al^{3+} or Fe^{3+} in the octahedral layer of laterite. In the region of 1,200–900 cm^{-1}, the bands in the region 1,004–794 cm^{-1} are due to the presence of Si–O–Fe, Al–OH, Fe–OH vibrations bands located at 794 and 910 cm^{-1} may be attributed to Si–O bonds linked with trivalent cations (e.g., Al^{3+}, Fe^{3+}). Thus, the presence of absorption bands at 794 and 910 cm^{-1} indicates the occurrence of tetrahedrally coordinated trivalent cations in laterite. The band at 540 cm^{-1} signifies the presence of Fe–O bond stretching [11].

It shows that the spectrum for RL and LD60 before adsorption are very similar to those after adsorption in both incidences (Figs. 1 and 2). This indicates that the main structures of both soil mixtures were not altered due to nitrate adsorption. Similar results have been obtained in studies carried out for nitrate adsorption using modified rice husk [36], and synthetic activated carbon magnetic nanoparticles [37].

Since there can be accumulated metal ions readily available in laterite soil samples, those metal ion concentrations needed to be analyzed. For this purpose, elution analysis was carried out for laterite. According to the results obtained Na, Mg, K, and Ca were the only elements present at ppm level (Table 3). All elements were present in levels that were highly below the WHO drinking water quality guidelines [9]. This concludes that the use of laterite to filter drinking water does not cause health risks due to the elution of heavy metals.

Detailed analyses of adsorption isotherms were conducted to compare the textural properties of fabricated materials (Fig. 3). The obtained isotherms of both samples are Type IV, according to the IUPAC report [38]. Type IV isotherms are given by mesoporous adsorbents. Mesoporous materials are materials that have an intermediate pore size range between 2–50 nm [39]. The adsorption behavior in mesopores is determined by the adsorbent–adsorptive interactions and also by the interactions between the molecules in the condensed state. In the case of Type IV isotherm, the initial monolayer-multilayer adsorption on the mesopore walls is followed by pore condensation.

The pore size distributions of LD60 and RL (Table 4) also confirm the significant presence of mesopores, as the recorded average pre radii of RL and LD60 were 3.81 and 3.82 nm,
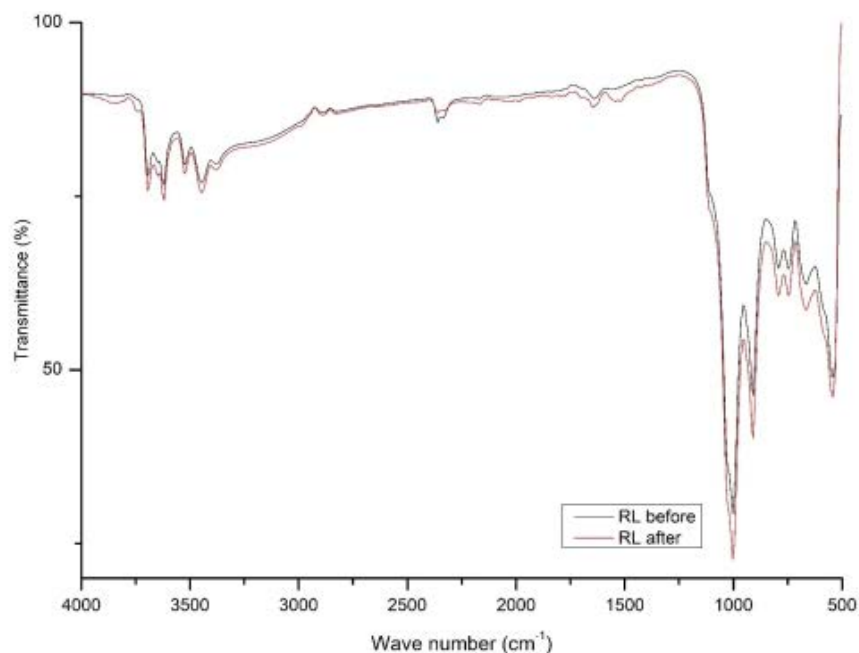
Fig. 1. Fourier-transform infrared spectroscopy for RL before and after nitrate adsorption.
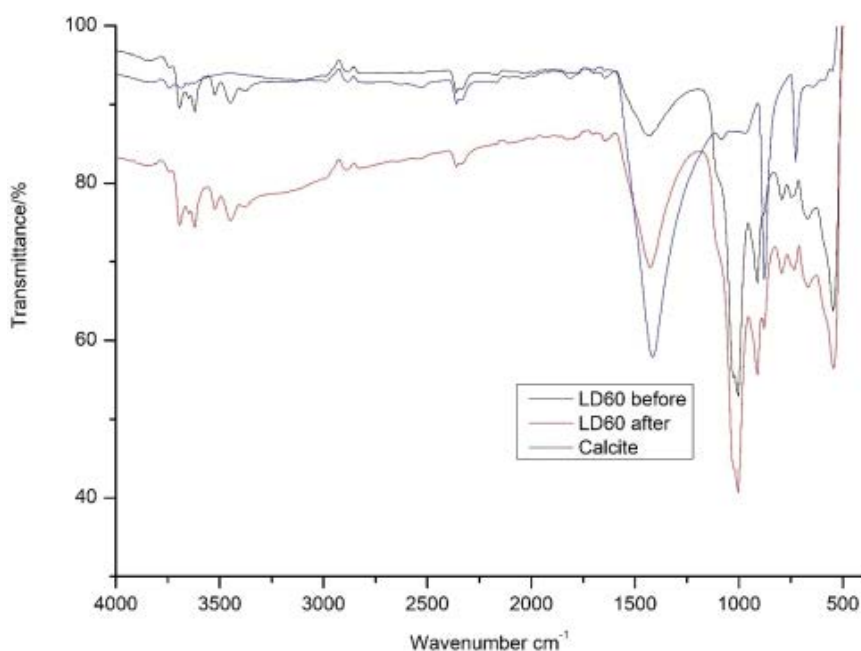

Fig. 2. Fourier-transform infrared spectroscopy for LD60 before and after nitrate adsorption.

respectively. Mesoporous materials have a number of key advantages that include narrow pore size distributions and high surface area, simple functionalization strategies with organics, biocompatibility, and low toxicity [39]. Therefore, it confirms the applicability of both mixtures for the study.

3.2. Batch experiments

Collected laterite and limestone samples were sieved to the smallest size of 0.5 mm and it has been shown in previous studies that as particle size decreases, particles are more prone to contamination and harder to decontaminate once the contaminant adsorption has taken place and thereby enhancing the adsorption process with the decrease in particle size [40]. Five replicates were used to determine the parameters.

3.2.1. Effect of laterite: limestone mixing ratio

As the optimum pH of nitrate adsorption for RL leads to acidic solutions, it was decided to amend the RL mixture

Table 3
Elements detected in the elution analysis

Element	Sample 1	Sample 2	Sample 3	Average	Min.	Max.	SD
Li/ppb	0.582	0.566	0.555	0.568	0.555	0.582	0.014
Be/ppb	0.001	0.000	0.049	0.017	0.000	0.049	0.028
Na/ppm	2.791	2.748	2.138	2.559	2.138	2.791	0.365
Mg/ppm	0.186	0.182	0.103	0.157	0.103	0.186	0.047
Al/ppb	20.494	17.084	23.828	20.469	17.084	23.828	3.372
K/ppm	1.008	0.984	0.000	0.664	0.000	1.008	0.575
Ca/ppm	5.323	5.042	0.000	3.455	0.000	5.323	2.995
Ti/ppb	13.760	14.149	0.000	9.303	0.000	14.149	8.059
V/ppb	0.156	0.101	0.110	0.122	0.101	0.156	0.030
Cr/ppb	0.160	0.000	0.000	0.053	0.000	0.160	0.092
Mn/ppb	5.509	4.652	0.000	3.387	0.000	5.509	2.964
Fe/ppb	23.345	7.320	0.000	10.222	0.000	23.345	11.94
Co/ppb	0.096	0.013	0.000	0.036	0.000	0.096	0.052
Ni/ppb	0.850	0.218	0.162	0.410	0.162	0.850	0.382
Cu/ppb	7.223	6.331	2.975	5.510	2.975	7.223	2.240
Zn/ppb	0.845	0.000	0.719	0.521	0.000	0.845	0.456
Ga/ppb	0.022	0.014	0.045	0.027	0.014	0.045	0.016
As/ppb	0.125	0.054	0.000	0.060	0.000	0.125	0.063
Se/ppb	2.995	2.983	0.000	1.993	0.000	2.995	1.726
Rb/ppb	4.954	4.876	0.000	3.277	0.000	4.954	2.838
Sr/ppb	16.083	15.886	0.000	10.656	0.000	16.083	9.229
Mo/ppb	0.027	0.147	0.176	0.117	0.027	0.176	0.079
Ag/ppb	0.000	0.000	0.051	0.017	0.000	0.051	0.029
Cd/ppb	0.000	0.000	0.000	0.000	0.000	0.000	0.000
In/ppb	0.001	0.001	0.051	0.018	0.001	0.051	0.029
Sn/ppb	0.043	0.187	0.227	0.152	0.043	0.227	0.097
Cs/ppb	0.425	0.422	0.044	0.297	0.044	0.425	0.219
Ba/ppb	3.437	2.912	0.000	2.116	0.000	3.437	1.852
Au/ppb	0.006	0.000	0.000	0.002	0.000	0.006	0.003
Au/ppb	0.001	0.000	0.000	0.000	0.000	0.001	0.001
Hg/ppb	0.070	0.000	0.000	0.023	0.000	0.070	0.040
205Tl	0.039	0.039	0.048	0.042	0.039	0.048	0.005
Pb/ppb	0.000	0.000	0.000	0.000	0.000	0.000	0.000
Bi/ppb	0.001	0.000	0.049	0.017	0.000	0.049	0.028
U/ppb	0.019	0.017	0.065	0.034	0.017	0.065	0.027

by mixing limestone powder. A nitrate solution of 25 mg/L concentration was used, and the mixtures were shaken for 24 h. The nitrate removal efficiency was determined using laterite-limestone mixtures prepared at different weight ratios, which included 50%, 60%, 70%, 80%, 90%, and 100% of laterite by weight.

The removal efficiency was the highest when LD60 was used, which includes 60% of laterite and 40% of limestone powder. The lowest removal efficiency was seen in LD60 which was made of 100% limestone powder (Fig. 4).

3.2.2. Effect of pH

Solution pH plays an important role in the adsorption of nitrate ions onto RL and LD60 because it can affect the surface charge and charging behavior of chemical speciation of nitrate. The initial pH of the solution varied from 2.0 to 11.0, and the effect on adsorption of the nitrate was determined. This ranged from 40.56% ± 1.76% and 63.04% ± 1.34% for RL and 42.72% ± 1.84% and 72.32% ± 2.68% for LD60 (Fig. 5). The optimum pH of both RL and LD60 was 3. Moreover, from the results, it was seen that at lower pH values, generally, the nitrate removal efficiency was higher than that at basic pH values. Similar results have been reported by other researchers who reported that adsorption of nitrate by other adsorbents was high at acidic pH and decreased at basic pH [37,41]. At lower pH, the negative surface charge of the adsorbent reduces due to the excess of protons in solutions. The decrease in pH of the system causes the number of positively charged sites of the adsorbent to increase.
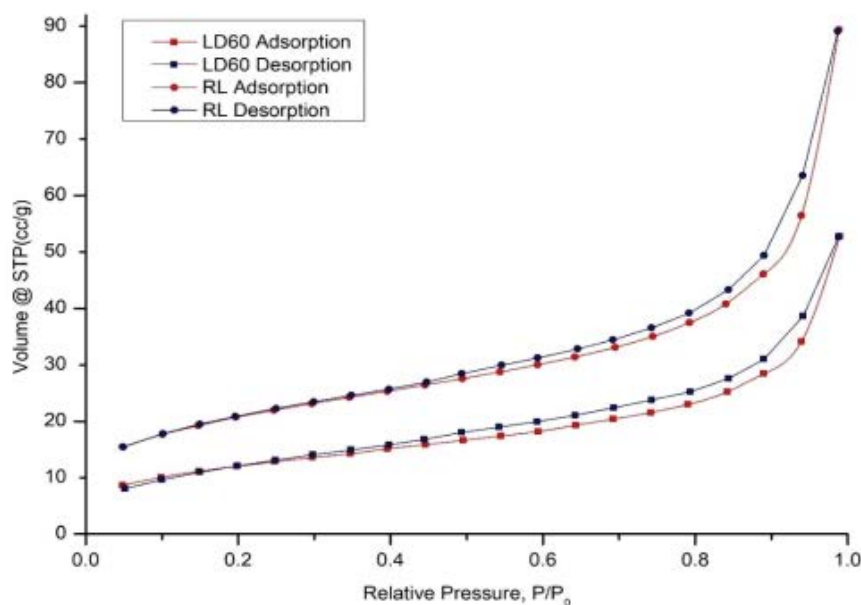
Fig. 3. Low temperature nitrogen adsorption and desorption isotherms of samples RL and LD60.

Table 4
Textural parameters of RL and LD60

Sample	Surface area (m^2/g)	Total pore volume (cm^3/g)	Average pore radius (nm)
RL	72.520	0.138	3.810
LD60	42.710	0.082	3.820

This can increase the electrostatic attraction between the surface of the soil and negatively charged nitrate ions which explains the removal of nitrate at such low pH. Naturally, positively charged surface sites on materials favor adsorption of nitrate anions due to electrostatic interactions [42].

In addition, as the pH increases, the hydroxide concentration to increases. The reduced removal efficiency can be due to higher competition between nitrate and hydroxide ions for the same sites on the adsorbent's surface. Nitrate and hydroxide may compete for the same sites on the adsorbent surface due to both species having similar charges [36].

Moreover, the point of zero charges (pH_{PZC}) was determined for laterite, and according to the results, the pH_{PZC} was calculated to be 6.70. The pH_{PZC} of laterite, according to previous studies, has been calculated as 3.98 [13], 7.40 [17]. When the pH of the solution is less than 6.70, the surface of laterite would be positive at pH values less than 6.70. In this situation, the adsorbent has a high ability to adsorb anionic species [24,41]. Nitrate being an anionic species,
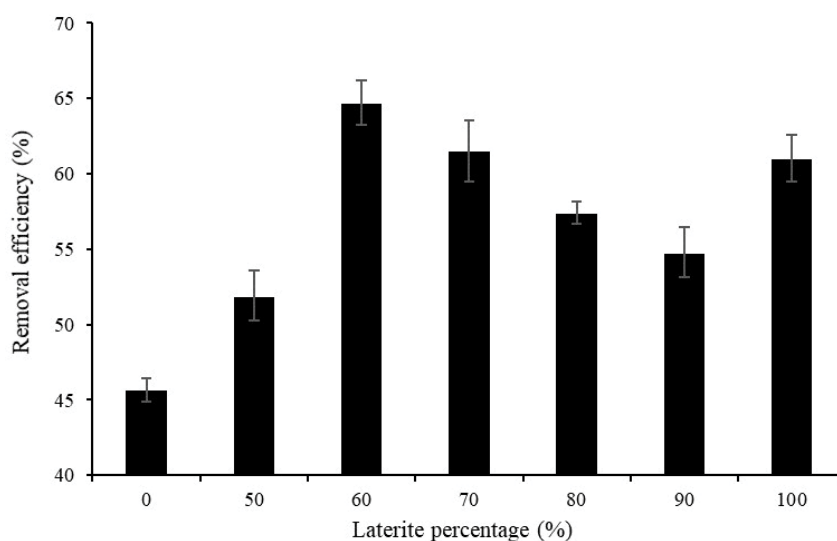

Fig. 4. Effect of laterite percentage in LD60 mixtures on the nitrate removal efficiency.

this confirms that the nitrate removal efficiency would be favored in acidic conditions.

When considering the variation of final pH with initial pH, LD60 showed more basic values than RL (Fig. 6). The reactivity of limestone in acid solutions has been extensively studied. The neutralization process can be described as the replacement of H^+ ions in the solution by Ca^{2+} present in the calcite of limestone [43]. As the final pH remains closer to neutral when using the laterite-limestone mixture, it is suitable for practical use as well.

3.2.3. Effect of dosage

Adsorbent dosage is another important factor that determines the optimum adsorbent dose, which is required to remove a definite amount of pollutants from the solution. In general, an increase in adsorbent dosage increases the adsorption of adsorbate from the solution due to the availability of more active sites and an increase in surface area at

a higher dosage [24]. It was evident that with the increase in adsorbent dosage from 0.5 to 10.0 g, the nitrate adsorption efficiency increased, and the adsorption capacity decreased (Fig. 7). The highest removal efficiency of RL was observed at laterite dosage of 2.5 g which was 58.96% ± 6.16%. Further increase in adsorbent dosage beyond 2.0 g did not significantly affect the nitrate adsorption capacity in both RL and LD60. Similar results were also reported by other researchers where nitrate adsorption efficiency from aqueous solution was found to increase up to the optimum dosage, and with further increase in adsorbent dose, the adsorption efficiency remained constant [42,44]. Therefore, based on the results of this study, the adsorbent dosage of 2.0 g was selected for both samples for further experiments.

3.2.4. Effect of contact time

The effect of contact time on nitrate adsorption capacity was conducted with the initial nitrate concentration of
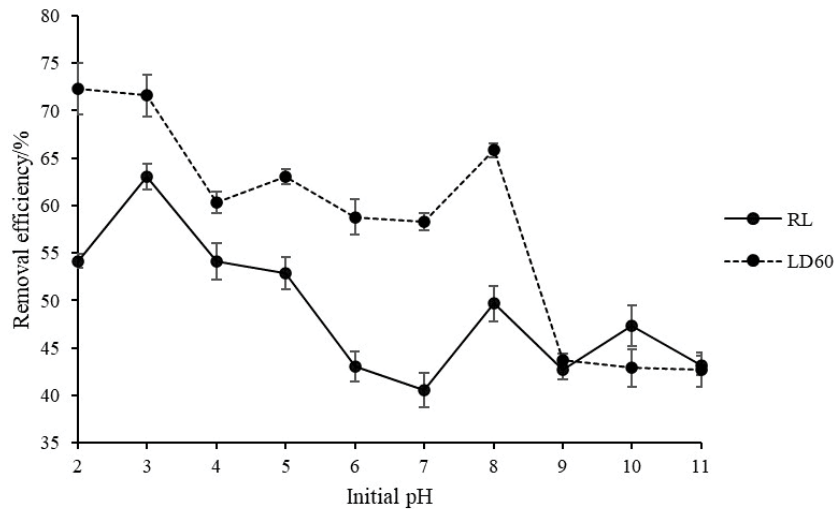

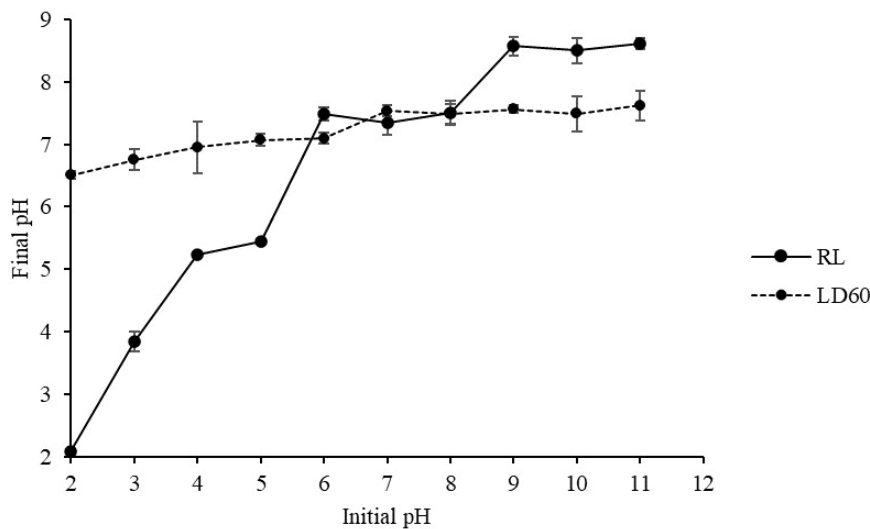Fig. 5. Variation of nitrate removal efficiency of RL and LD60 with changes in initial pH.

Fig. 6. Variation of final pH with initial pH.

25 mg/L, the adsorbent dosage of 2.0 g, and an optimum initial pH of 3. It was found that the removal efficiency of both mixtures for removing nitrate was rapid in the beginning stages of contact time (Fig. 8). The highest removal efficiency of RL was observed at 24 h which was 56.32% ± 0.59%. After 20 min, the rate of adsorption decreases with time, and the adsorption process reaches equilibrium within 60 min. This phenomenon might be due to the presence of a greater number of active sites for the adsorption of nitrate ions during the initial stages. According to the obtained results, a contact time of 60 min for RL and 180 min for LD60 was chosen for further experiments. The results of contact time show that the process of nitrate adsorption is comparable with other adsorbents studied by researchers, such as graphene and modified sugarcane bagasse biochar [24,41].

3.2.5. Adsorption kinetic studies

When considering the results of RL, as shown in the plot of ln $(q_e - q_t)$ vs. time gives a higher R^2 of 0.987 for RL,

suggesting that it follows pseudo-first-order kinetics (Fig. 9). It indicates that the reaction is more inclined towards physisorption. The experimental q_e value of RL is seen to be comparatively close to the calculated q_e value in the pseudo-first-order model, which further suggests the compatibility of the said model over other kinetic models for RL (Table 5).

Considering LD60, the plot of t/q_t vs. time gives an R^2 of 0.996, suggesting it follows pseudo-second-order kinetics (Fig. 10). A good fit of experimental data with the pseudo-second-order model would indicate that chemical adsorption is the rate-controlling mechanism. This suggests that the rate-limiting step may involve valency forces by sharing or exchanging electrons between sorbent and sorbate [29]. Similar results have also been reported by other researchers where the pseudo-second-order kinetic model has shown good agreement with the experimental data for adsorption of nitrate ions [24]. The observed q_e value of LD60 is seen to be comparatively close to the calculated q_e value in the pseudo-second-order model, which further suggests the compatibility of the said model over other kinetic models for LD60.
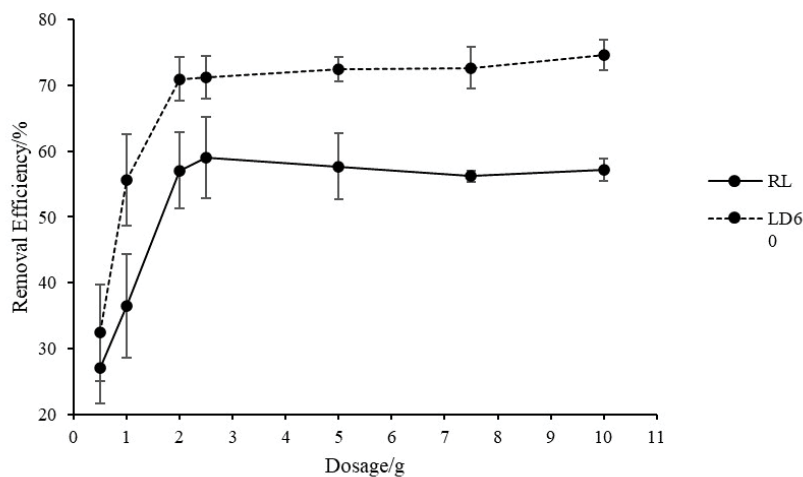

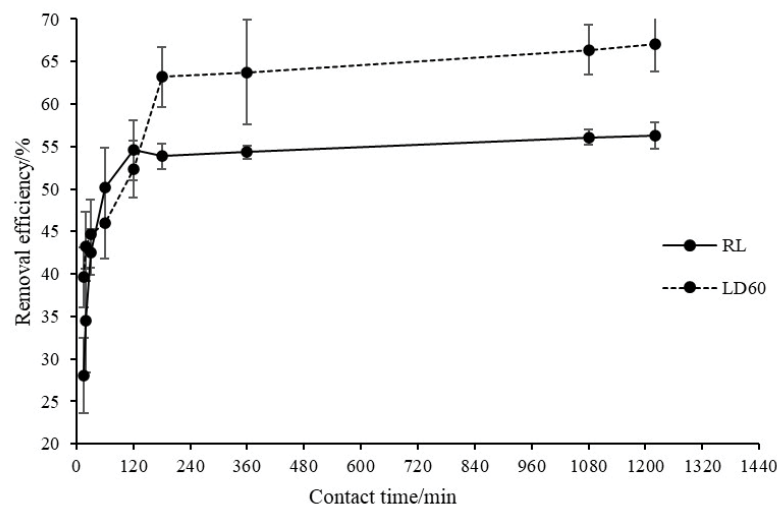Fig. 7. Variation of nitrate removal efficiency with RL and LD60 dose.

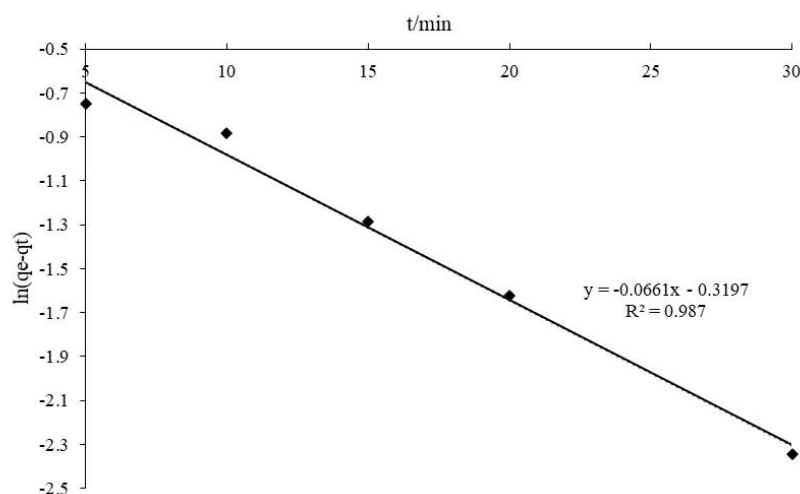Fig. 8. Variation of nitrate removal efficiency of RL and LD60 with contact time.

Fig. 9. Pseudo-first-order kinetic model for the nitrate adsorption by RL.

Table 5
Kinetic parameters for nitrate adsorption by RL and LD60

Kinetic model	Parameter	RL	LD60
Pseudo-first-order	R^2	0.987	0.892
	k_1 (min^{-1})	0.066	0.007
	q_e (cal) (mg/g)	0.726	0.326
	q_e (exp) (mg/g)	0.682	0.790
Pseudo-second-order	R^2	0.960	0.996
	k_2 (g/mg·min)	0.042	0.298
	q_e (cal) (mg/g)	0.918	0.668
	q_e (exp) (mg/g)	0.682	0.790
Intraparticle diffusion	R^2	0.928	0.883
	K_p (mg/g·min$^{0.5}$)	10.28	0.023
	I (mg/g)	0.533	0.406

3.2.6. Adsorption isotherms

The adsorption characteristic equilibrium studies of prepared materials for nitrates removal from aqueous solutions were investigated. Three adsorption models fitted the experimental data, and the Langmuir adsorption isotherm showed the best fit to the experimental data of RL with R^2 of 0.981 (Fig. 11). Therefore, the adsorption can be mainly controlled by monolayer adsorption [32].

In mixture LD60, the experimental data fitted the Freundlich adsorption isotherm (Fig. 12) with an R^2 of 0.987, which means multilayer adsorption played a dominant role [45]. The n value in the Freundlich model is 1.305 (Table 6), which indicates favorable adsorption of nitrate by the LD60 [24]. Similar results have been seen in studies carried out on the removal of nitrate [39].

3.2.7. Effect of competing ions

It was found that the adsorption capacity of LD60 towards nitrate was reduced due to the presence of co-existing (phosphate, fluoride, and sulfate) in the water. Fluoride and sulfate showed almost equal effects on nitrate adsorption, and the removal efficiency ranged between 41.20% ± 1.47% to 46.32% ± 1.634% in the presence of fluoride and between 43.84% ± 1.04% to 39.68% ± 1.37% in the presence of sulfate (Fig. 13). As the concentration of the competing ion increased, the nitrate removal efficiency decreased. It could be explained by the fact that in multi-element solutions, the electrostatic interaction of co-existing anions with adsorption sites of soil was much stronger than nitrate ions species. Phosphate ions have shown maximum effects on the adsorption of nitrate, and the removal efficiency varied between 35.12% ± 3.48% to 38.08% ± 1.07%. It has been reported that multivalent anion with higher charge density was adsorbed more readily than monovalent anions [37]. Other researchers have reported similar results where multivalent, and mono charge anions have shown more and less adsorption trend, respectively [24,37].

The negatively charged surfaces of the laterite soil particles can attract and retain nitrate ions when they are present in the solution. The electrostatic forces between the negatively charged nitrate ions and the positively charged sites on the surface of the soil particles are what cause this attraction [33,39]. The nitrate ions go through a process known as adsorption as they come into contact with the laterite soil. The nitrate ions attach to the surfaces of soil particles during adsorption, creating a thin layer of nitrate molecules [33,39]. In order to remove nitrate from the solution, this interaction is crucial. Numerous sites for nitrate adsorption can be found in the laterite soil due to its large surface area and wealth of clay minerals [11].

Laterite soil is naturally rich in iron and aluminum compounds, which increases its stability. A solid structure is created by the interlocking and compact packing of the soil particles [11]. Due to its high resistance to erosion, laterite soil is particularly advantageous in regions with frequent heavy rain or strong winds. As a result of its strength, it is an excellent material for building foundations, highways, and even houses. The ability of laterite soil to be recycled is one of its remarkable qualities. It is possible for laterite soil to go through a process known as stabilization when it is excavated or dug up for construction. To enhance its
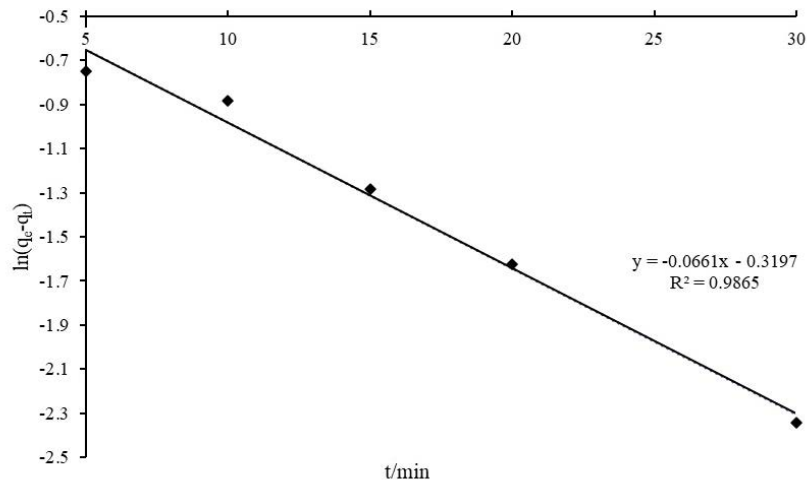
Fig. 10. Pseudo-second-order kinetic model for the nitrate adsorption by LD60.
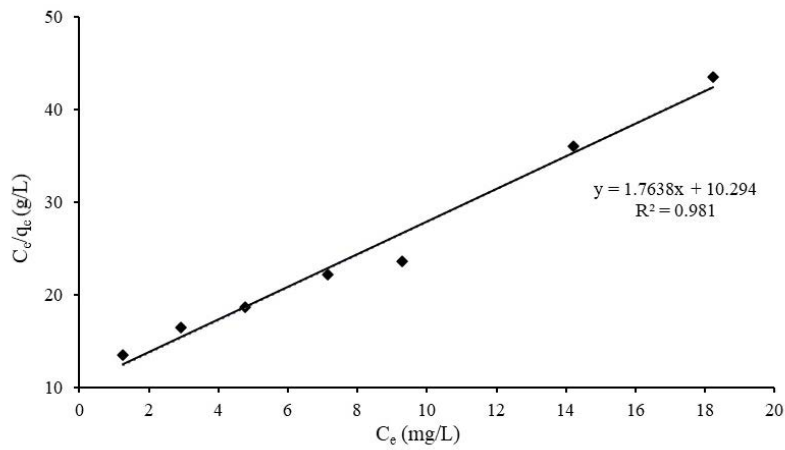

Fig. 11. Langmuir isotherm showing the variation of adsorption (C_e/q_e) against the equilibrium concentration (C_e) for adsorption of nitrate ions onto RL.
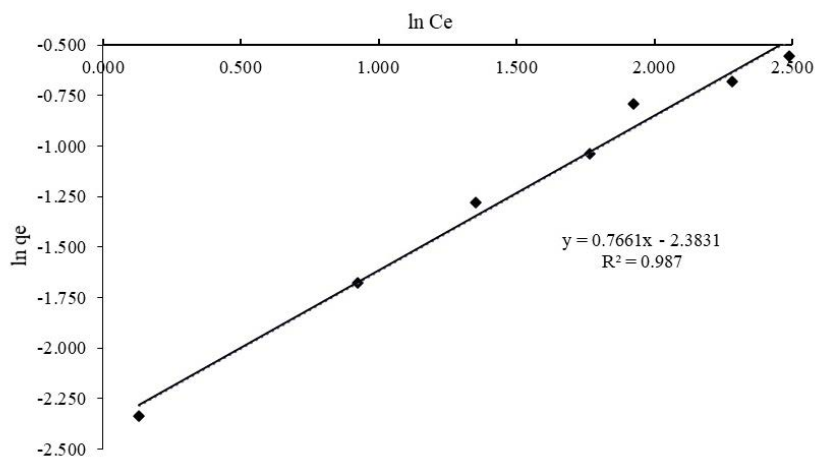

Fig. 12. Freundlich isotherm showing the variation of $\ln q_e$ against $\ln C_e$ for adsorption of nitrate ions onto LD60.

engineering properties, stabilization involves adding addi- tives like cement, lime, or fly ash [11,12]. This procedure increases the strength and durability of laterite soil, enabling its reuse in construction projects. Recycling laterite soil reduces waste and the need to mine new resources, making it an environmentally friendly choice.
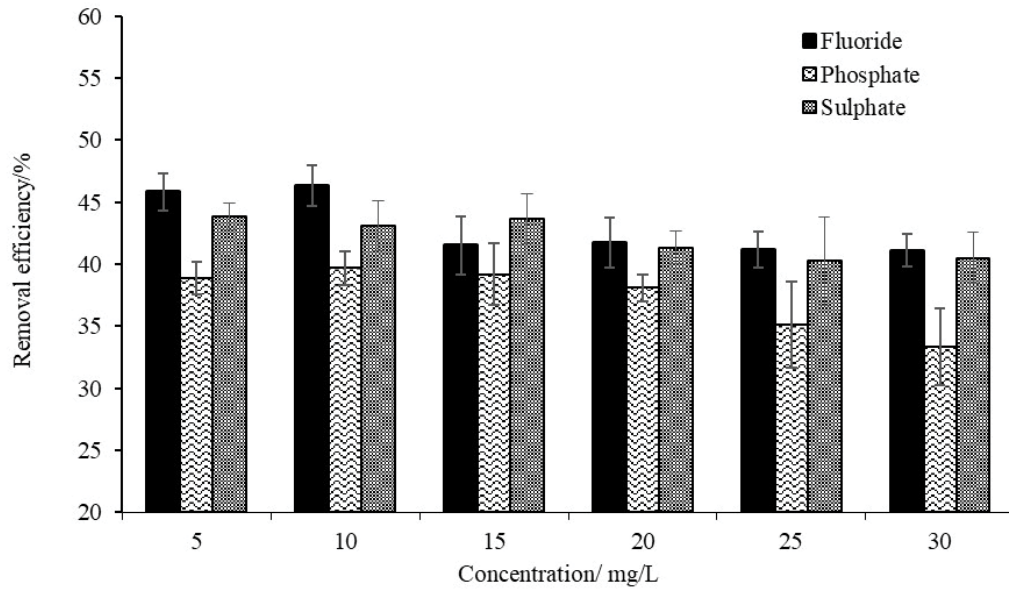
Fig. 13. Effect of competing anions on adsorption capacity of LD60 for nitrate adsorption.
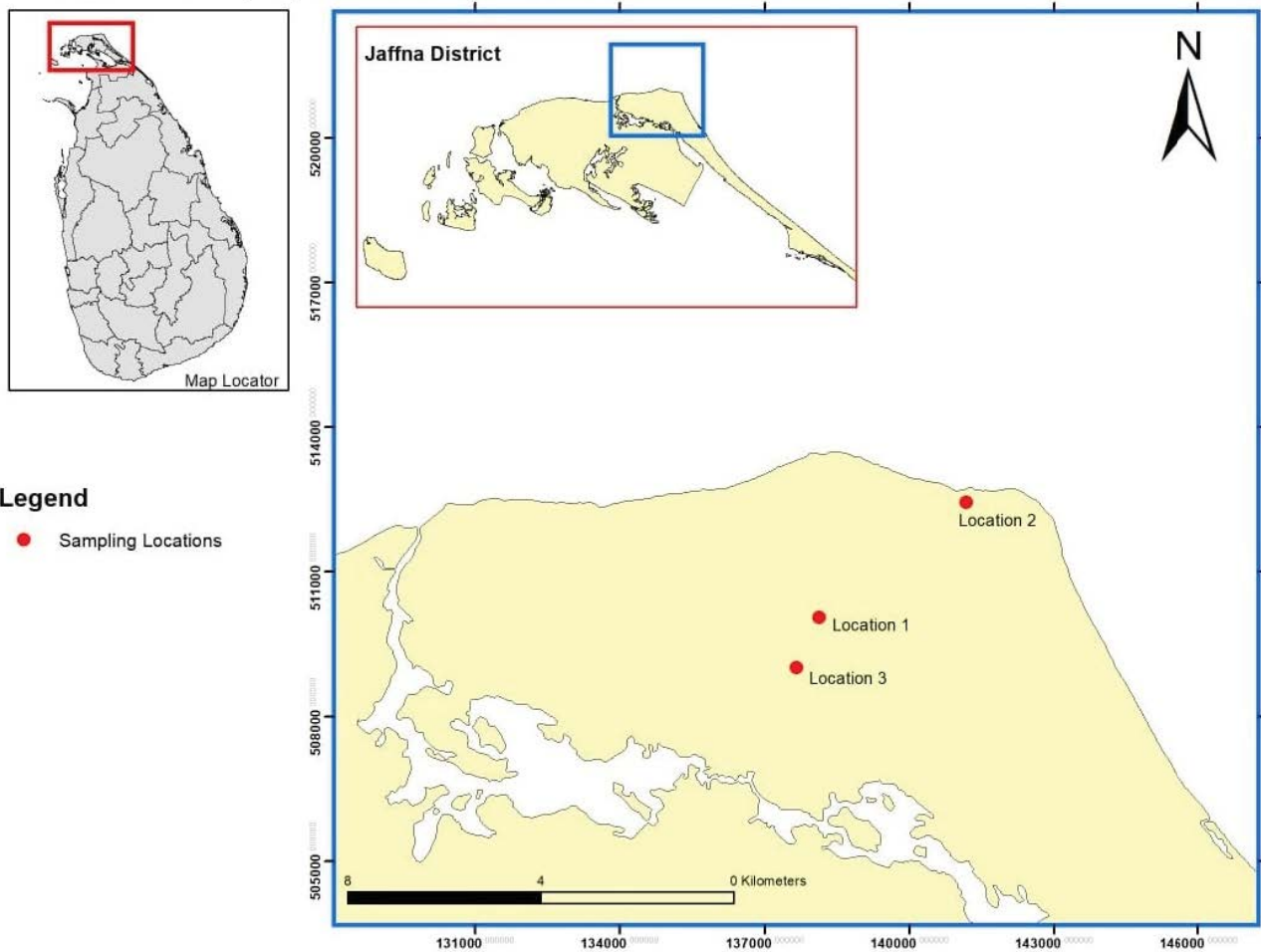

Fig. 14. Groundwater collection sites in Jaffna district.

Table 6
Langmuir, Freundlich and Temkin isotherm parameters for adsorption of nitrate on RL and LD60

Isotherm	Parameter	RL	LD60
Langmuir	R^2	0.981	0.951
	Q_0	0.567	1.212
	K_L	0.171	0.076
Freundlich	R^2	0.944	0.987
	N	1.745	1.305
	K_F	0.094	0.092
Temkin	R^2	0.968	0.962
	B	334.120	534.090
	A_t	0.950	0.985

4. Conclusion

The results of this study suggest that, laterite soil and laterite-limestone mixtures are effective adsorbents for nitrate adsorption from aqueous solutions. Laterite soil was mesoporous and is suitable to be used as an adsorbent. Nitrate adsorption efficiency was higher under acidic pH as compared to basic pH. The adsorption studies were investigated by batch method, and maximum removal was obtained at pH 3. The results showed that adsorption equilibrium was reached within 60 and 180 min, respectively, for RL and LD60. The maximum adsorption capacity of laterite soil for nitrate ions was obtained as 0.628 mg/g.

Acknowledgment

References

[1] S. Velizarov, J.G. Crespo, M.A. Reis, Removal of inorganic anions from drinking water supplies by membrane bio/processes, Rev. Environ. Sci. Bio/Technol., 3 (2004) 361–380.
[2] T. Thompson, Supplies in Saskatchewan, Canada, Bull. Environ. Contam. Toxicol., 66 (2001) 64–70.
[3] A. Bhatnagar, M. Sillanpää, A review of emerging adsorbents for nitrate removal from water, Chem. Eng. J., 168 (2011) 493–504.
[4] G. Luk, W. Au-Yeung, Experimental investigation on the chemical reduction of nitrate from groundwater, Adv. Environ. Res., 6 (2002) 441–453.
[5] V. Jeevaratnam, S. Balakumar, T. Mikunthan, M. Prabaharan, Quality of groundwater in Valikamam area, Jaffna Peninsula, Sri Lanka, Int. J. Water Res. Environ. Eng., 10 (2018) 9–16.
[6] S. Suthar, P. Bishnoi, S. Singh, P.K. Mutiyar, A.K. Nema, N.S. Patil, Nitrate contamination in groundwater of some rural areas of Rajasthan, India, J. Hazard. Mater., 171 (2009) 189–199.
[7] X.T. Ju, C.L. Kou, F.S. Zhang, P. Christie, Nitrogen balance and groundwater nitrate contamination: comparison among three intensive cropping systems on the North China Plain, Environ. Pollut., 143 (2006) 117–125.
[8] M.H. Ward, R.R. Jones, J.D. Brender, T.M. De Kok, P.J. Weyer, B.T. Nolan, C.M. Villanueva, S.G. van Breda, Drinking water nitrate and human health: an updated review, Int. J. Environ. Res. Public Health, 15 (2018) 1557, doi: 10.3390/ijerph15071557.
[9] W. Weber, J. Morris, Intraparticle diffusion during the sorption of surfactants onto activated carbon, J. Sanit. Eng. Div. Am. Soc. Civ. Eng., 89 (1963) 53–61.
[10] C. Dissanayake, Mineralogy and chemical composition of some laterites of Sri Lanka, Geoderma, 23 (1980) 147–155.
[11] S. Mitra, L.S. Thakur, V.K. Rathore, P. Mondal, Removal of Pb(II) and Cr(VI) by laterite soil from synthetic wastewater: single and bi-component adsorption approach, Desal. Water Treat., 57 (2016) 18406–18416.
[12] R. Ranasinghe, D. Werellagama, R. Weerasooriya, Arsenite removal from drinking water using naturally available laterite in Sri Lanka, J. Inst. Eng. (Sri Lanka), 47 (2014) 23–31.
[13] M. Sarkar, A. Banerjee, P.P. Pramanick, A.R. Sarkar, Use of laterite for the removal of fluoride from contaminated drinking water, J. Colloid Interface Sci., 302 (2006) 432–441.
[14] M. Vithanage, L. Jayarathna, A.U. Rajapaksha, C.B. Dissanayake, M.S. Bootharaju, T. Pradeep, Modeling sorption of fluoride on to iron rich laterite, Colloids Surf., A, 398 (2012) 69–75.
[15] N.U.S. Dissanayake, P.H. Pupulewatte, D.T. Jayawardana, Thermally activated laterite soil as an adsorbent for phosphate and fluoride removal from contaminated water, Desal. Water Treat., 270 (2022) 227–235.
[16] L. Zhang, S. Hong, J. He, F. Gan, Y.S. Ho, Adsorption characteristic studies of phosphorus onto laterite, Desal. Water Treat., 25 (2011) 98–105.
[17] T.D. Pham, H.H. Nguyen, N.V. Nguyen, T.T. Vu, T.N.M. Pham, T.H.Y. Doan, M.H. Nguyen, T.M.V. Ngo, Adsorptive removal of copper by using surfactant modified laterite soil, J. Chem., 2017 (2017) 1986071, doi: 10.1155/2017/1986071.
[18] N.U.S. Dissanayake, D.T. Jayawardana, S. Buddhima, H. Mapatuna, H. Ravilojan, Thermally modified laterite soil by means of an adsorptive material for copper and chromium elimination from polluted water, Chem. Environ. Sci. Arch., 3 (2023) 8–14.
[19] P.G. Cooray, An Introduction to the Geology of Sri Lanka (Ceylon), National Museums of Sri Lanka Publication, 1984.
[20] M.M.M.G.P.G. Mantilaka, H.M.T.G.A. Pitawala, R.M.G. Rajapakse, D.G.G.P. Karunaratne, Nanomaterials From Sri Lankan Marble: A Novel Approach for Value Added Products, Annual Sessions, Geological Society, Colombo, Sri Lanka, 2013.
[21] E. Iakovleva, M. Sillanpää, P. Maydannik, J.T. Liu, S. Allen, A.B. Albadarin, C. Mangwandi, Manufacturing of novel low-cost adsorbent: co-granulation of limestone and coffee waste, J. Environ. Manage., 203 (2017) 853–860.
[22] S. Maeda, A. Ohki, S. Saikoji, K. Naka, Iron(III) hydroxide-loaded coral limestone as an adsorbent for arsenic(III) and arsenic(V), Sep. Sci. Technol., 27 (1992) 681–689.
[23] N.A. Akbar, H.A. Aziz, M.N. Adlan, Potential of high quality limestone as adsorbent for iron and manganese removal in groundwater, Jurnal Teknologi, 78 (2016), doi: 10.11113/jt.v78.9700.
[24] L.D. Hafshejani, A. Hooshmand, A.A. Naseri, A.S. Mohammadi, F. Abbasi, A. Bhatnagar, Removal of nitrate from aqueous solution by modified sugarcane bagasse biochar, Ecol. Eng., 95 (2016) 101–111.
[25] I.V.K. Nayanthika, D.T. Jayawardana, N.J.G.J. Bandara, P.M. Manage, R.M.T.D. Madushanka, Effective use of iron-aluminum rich laterite-based soil mixture for treatment of landfill leachate, Waste Manage., 74 (2018) 347–361.
[26] N.U.S. Dissanayake, P.G.H. Pupulewatte, D.T. Jayawardana, D.M. Senevirathne, Characterization of kaolin-rich laterite soil for applications for the development of soil-based cosmetic products, J. Drug Delivery, 12 (2022) 31–40.
[27] A. Rahmani, H.Z. Mousavi, M. Fazli, Effect of nanostructure alumina on adsorption of heavy metals, Desalination, 253 (2010) 94–100.
[28] S.K. Lagergren, About the theory of so-called adsorption of soluble substances, Sven. Vetenskapsakad. Handingarl., 24 (1898) 1–39.
[29] A. Aurich, J. Hofmann, R. Oltrogge, M. Wecks, R. Gläser, L. Blömer, S. Mauersberger, R.A. Müller, D. Sicker, A. Giannis,

Improved isolation of microbiologically produced (2R,3S)-isocitric acid by adsorption on activated carbon and recovery with methanol, Org. Process Res. Dev., 21 (2017) 866–870.

[30] H. Freundlich, Over the adsorption in solution, J. Phys. Chem., 57 (1906) 1100–1107.

[31] D.G. Kinniburgh, General purpose adsorption isotherms, J. Environ. Sci. Technol., 20 (1986) 895–904.

[32] I. Langmuir, The constitution and fundamental properties of solids and liquids. Part I. Solids, J. Am. Chem. Soc., 38 (1916) 2221–2295.

[33] M. Mahagamage, S. Pavithrani, M. Pathmalal, Water quality and microbial contamination status of groundwater in Jaffna Peninsula, Sri Lanka, J. Water Land Dev., (2019), doi: 10.2478/jwld-2019-0001.

[34] M. Vithanage, T. Mikunthan, S. Pathmarajah, S. Arasalingam, H. Manthrithilake, Assessment of nitrate-N contamination in the Chunnakam aquifer system, Jaffna Peninsula, Sri Lanka, SpringerPlus, 3 (2014) 1–8.

[35] A. Maiti, B.K. Thakur, J.K. Basu, S. De, Comparison of treated laterite as arsenic adsorbent from different locations and performance of best filter under field conditions, J. Hazard. Mater., 262 (2013) 1176–1186.

[36] R. Katal, M.S. Baei, H.T. Rahmati, H. Esfandian, Kinetic, isotherm and thermodynamic study of nitrate adsorption from aqueous solution using modified rice husk, J. Ind. Eng. Chem., 18 (2012) 295–302.

[37] R. Rezaei Kalantary, E. Dehghanifard, A. Mohseni-Bandpi, L. Rezaei, A. Esrafili, B. Kakavandi, A. Azari, Nitrate adsorption by synthetic activated carbon magnetic nanoparticles: kinetics, isotherms and thermodynamic studies, Desal. Water Treat., 57 (2016) 16445–16455.

[38] M. Thommes, K. Kaneko, A.V. Neimark, J.P. Olivier, F. Rodriguez-Reinoso, J. Rouquerol, K.S.W. Sing, Physisorption of gases, with special reference to the evaluation of surface area and pore size distribution (IUPAC Technical Report), Pure Appl. Chem., 87 (2015) 1051–1069.

[39] Z. Wu, D. Zhao, Ordered mesoporous materials as adsorbents, Chem. Commun., 47 (2011) 3332–3338.

[40] H. Wang, F. Shadman, Effect of particle size on the adsorption and desorption properties of oxide nanoparticles, AlChE J., 59 (2013) 1502–1510.

[41] P. Ganesan, R. Kamaraj, S. Vasudevan, Application of isotherm, kinetic and thermodynamic models for the adsorption of nitrate ions on graphene from aqueous solution, J. Taiwan Inst. Chem. Eng., 44 (2013) 808–814.

[42] E. Viglašová, M. Galamboš, Z. Danková, L. Krivosudský, C.L. Lengauer, R. Hood-Nowotny, G. Soja, A. Rompel, M. Matík, J. Briančin, Production, characterization and adsorption studies of bamboo-based biochar/montmorillonite composite for nitrate removal, J. Waste Manage., 79 (2018) 385–394.

[43] P. Barton, T. Vatanatham, Kinetics of limestone neutralization of acid waters, J. Environ. Sci. Technol., 10 (1976) 262–266.

[44] Y. Yao, B. Gao, M. Zhang, M. Inyang, A.R. Zimmerman, Effect of biochar amendment on sorption and leaching of nitrate, ammonium, and phosphate in a sandy soil, Chemosphere, 89 (2012) 1467–1471.

[45] M.B. Desta, Batch sorption experiments: Langmuir and Freundlich isotherm studies for the adsorption of textile metal ions onto teff straw (*Eragrostis tef*) agricultural waste, J. Thermodyn., 2013 (2013) 375830, doi: 10.1155/2013/375830.